

CO₂ Hydrogenation Mechanism on Graphene-supported Subnanometer Ni₇ Cluster

Adhitya Gandaryus Saputro^{a,b,*}, Mochammad Rizky Pradana^a, Arifin Luthfi Maulana^a, Mohammad Kemal Agusta^{a,b}, and Hermawan Kresno Dipojono^{a,b}

Received

31 May 2021

Accepted

28 June 2021

Published

21 July 2021

DOI: 10.5614/jrdn/2021.1.1.16425

We study the mechanism of carbon dioxide (CO₂) hydrogenation to carbon monoxide (CO) and formic acid (HCOOH) on a graphene-supported subnanometer Ni₇ cluster by means of density functional theory calculations. We find that this system has similar activation energies for the first CO₂ hydrogenation step for the formate and the reverse water-gas shift (RWGS) pathways. However, the second hydrogenation step for these pathways has very distinct profiles. The HCOOH formation on the formate pathway has very large activation energy, while the CO formation on the RWGS pathway has negligible activation energy. We conclude that the CO₂ hydrogenation process on this system is more selective towards the RWGS pathway to produce CO.

Keywords: CO₂ hydrogenation; CO; formic acid; density functional theory; graphene; subnanometer Ni cluster.

Introduction

Direct conversion of CO₂ molecules into valuable chemicals through the hydrogenation process is a beneficial scheme that can help to mitigate the excessive CO₂ emission in our atmosphere (Abanades *et al.*, 2017; Álvarez *et al.*, 2017; Kätelhön *et al.*, 2019; Mustafa *et al.*, 2020). Unfortunately, the current technology for converting CO₂ through a hydrogenation scheme still involves a very energy-intensive process (Waugh, 1992; Liu *et al.*, 2003). This process needs high-temperature and high-pressure conditions to facilitate the chain of complex hydrogenation reactions that require high activation energies. The development of catalyst material that can significantly facilitate this hydrogenation process is urgently needed.

Nickel (Ni) surface has been widely applied as a catalyst for various chemical processes (Mahyuddin *et al.*, 2016; Agusta *et al.*, 2017, 2019; Mahyuddin and Yoshizawa, 2018; Singha *et al.*, 2019; Zhang *et al.*, 2019). However, this surface cannot be adequately applied as an effective CO₂ hydrogenation catalyst due to its weak interaction with the inert CO₂ molecule (Remediakis, Abild-Pedersen and Nørskov, 2004; Wang *et al.*, 2005; X. Ding *et al.*, 2007; Xunlei Ding *et al.*, 2007; Vesselli *et al.*, 2008, 2010; Catapan *et al.*, 2012; Peng *et al.*, 2012; Nugraha *et al.*, 2016; Maulana *et al.*, 2019). Strong interaction between catalyst and CO₂ is a necessary condition to activate the inert CO₂ molecule. Therefore, a geometrical modification of the flat Ni surface might be necessary if we want to try to apply it as a CO₂ hydrogenation catalyst (Saputro *et al.*, 2016, 2019; Saputro and Akbar, 2017; Saputro, Maulana, Aprilyanti, *et al.*, 2021; Saputro, Maulana, Fathurrahman, *et al.*, 2021).

We previously studied the adsorption of a CO₂ molecule on a graphene-supported subnanometer Ni_x cluster (Pradana *et al.*, 2019). The structural transition from a bulk Ni surface to a very small subnanometer Ni_x cluster significantly modifies the Ni-CO₂ interaction. The small Ni_x cluster can strongly adsorb the CO₂ molecule with a bidentate adsorption configuration. The formation of bidentate configuration weakens the internal C-O bonds of the adsorbed CO₂ molecule, making it ready to undergo a chemical reaction. Such a condition suggests that the subnanometer Ni_x cluster might be able to facilitate the CO₂ hydrogenation process.

In this work, we study the atomic-scale mechanism of CO₂ hydrogenation reaction to CO and formic acid (HCOOH) on graphene-supported subnanometer Ni₇ cluster by means of the density functional theory calculations. This hydrogenation mechanism is very important to understand the catalytic properties of the subnanometer Ni_x catalyst.

Computational Details

All of spin-polarized density functional theory (Hohenberg and Kohn, 1964; Kohn and Sham, 1965) calculations are performed using Quantum Espresso package (Giannozzi *et al.*, 2009). Exchange and correlation functional are described by generalized gradient approximation using the Perdew-Burke-Ernzerhof (PBE) functional (Perdew, Burke and Ernzerhof, 1996). Ultrasoft pseudopotentials are used to describe the interaction between valence electrons and the ion core. DFT-D2 was used to describe the van der Waals interaction (Grimme, 2006). The value of cutoff for plane-wave and electronic densities are 30 Ry and 360 Ry, respectively. The Brillouin zone sampling for the calculation of the isolated Ni₇ cluster, CO₂, CO, H₂, and HCOOH is simulated using gamma point, while the calculation for the rest is carried out using 2 × 2 × 1 k-points. The total energy of the Ni₇ cluster and isolated molecules are computed in a 30 Å × 30 Å × 30 Å unit cell.

^aAdvanced Functional Materials Research Group, Institut Teknologi Bandung, Jl. Ganesha 10, Bandung 40132, Indonesia

^bResearch Center for Nanosciences and Nanotechnology, Institut Teknologi Bandung, Jl. Ganesha 10, Bandung 40132, Indonesia

* Corresponding author: ganda@tf.itb.ac.id

We previously found that a pristine graphene layer can properly fixate a subnanometer Ni_x cluster on its surface (Pradana *et al.*, 2019). However, the presence of graphene does not affect the cluster interaction with a CO_2 molecule. It suggests that pristine graphene is a good support model for studying the innate catalytic activity of a supported subnanometer metal cluster. In this study, we use a 5×5 graphene to model a graphene-supported subnanometer Ni_7 cluster ($Ni_7/Graphene$). The size of the graphene sheet is adequate to support the Ni_7 cluster and to minimize the interaction with other Ni_7 clusters on the adjacent unit cells. The Ni_7 cluster is chosen to represent the subnanometer Ni_x cluster model because it can provide enough adsorption sites for the simultaneous adsorption of CO_2 -related molecules and H atoms. We also added a vacuum space of 15 \AA in the z-direction to minimize the interaction between repeated surface slabs. The model of $Ni_7/Graphene$ super cell is presented in **Fig. 1**.

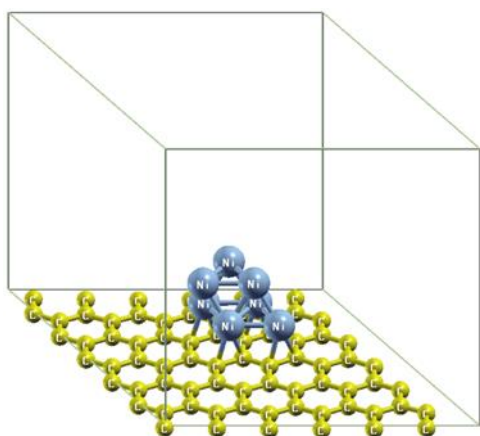


Figure 1. Super cell model graphene-supported subnanometer Ni_7 cluster

Geometry optimizations are performed without any geometrical constraint. Energy barriers of an elementary reaction are calculated using the nudged elastic band method (NEB) (Henkelman, Uberuaga and Jónsson, 2000). The activation energy of an elementary reaction (E_a) is calculated using the following relation,

$$E_a = E^{TS} - E^{IS}, \quad (1)$$

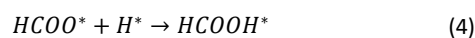
where E^{IS} and E^{TS} represent the total energy of the initial state (IS) and the transition state (TS), respectively. Reaction energy of an elementary reaction is calculated as,

$$\Delta E = E^{FS} - E^{IS} \quad (2)$$

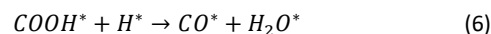
where E^{FS} represents the final state (FS) of the reaction.

Results and Discussion

The CO_2 hydrogenation to $HCOOH$ consists of the following elementary reactions:



These reactions are known as the formate pathway. X^* represents an adsorbed X species on the Ni_7 cluster. The CO_2 hydrogenation to CO consists of the following elementary reactions:



These reactions are known as the reverse water-gas shift (RWGS) pathway.

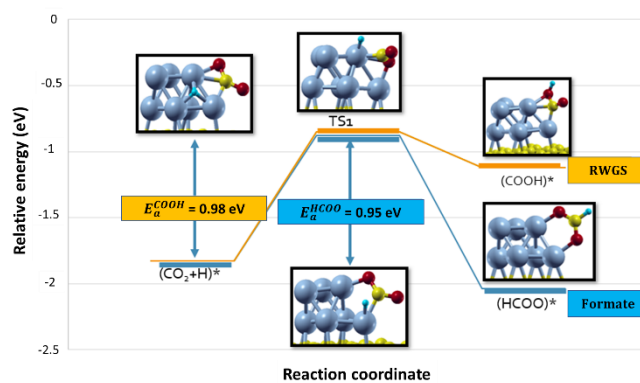


Figure 2. Initial state (IS), transition state (TS), and final state (FS) of the first hydrogenation step.

Both formate and RWGS pathways start from an identical initial state, as shown in **Fig. 2**. In the case of $HCOO$ formation, the H atom attacks the C atom of the adsorbed CO_2 in the case of $HCOO$ formation, while it attacks one of the O atoms of the adsorbed CO_2 in the case of $COOH$ formation. The activation energies for these two reactions only differs by 0.02 eV ($E_a^{HCOO} = 0.95 \text{ eV}$ and $E_a^{COOH} = 0.98 \text{ eV}$). The $COOH$ formation has slightly higher activation energy since the reaction energy of this elementary step is more endothermic than the $HCOO$ formation, in agreement with the Brønsted-Evans-Polanyi (BEP) relation (Bronsted, 1928; Evans and Polanyi, 1938).

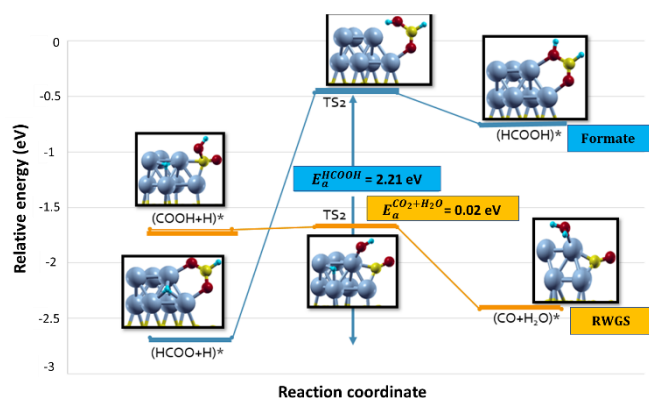


Figure 3. Initial state (IS), transition state (TS), and final state (FS) of the second hydrogenation step.

The energy profiles for the second hydrogenation step for the formate and RWGS are quite different from the initial step, as presented in **Fig. 3**. In the case of HCOOH* formation, the adsorbed H atom attacks one of the O atoms of the HCOO*. This process requires quite high activation energy, $E_a^{HCOOH} = 2.21$ eV. Such high activation energy suggests that the formation of HCOOH through the formate pathway might not be energetically feasible on this catalyst. In the case of CO formation, the COOH* is dissociated into CO* and OH*, and the adsorbed H atom simultaneously attacks the OH* to form H₂O*. Interestingly, the required activation energy for this process is practically negligible, $E_a^{CO_2+H_2O} = 0.02$ eV. This value shows that the Ni₇ cluster can greatly facilitate the dissociation of COOH*. Once again, the second hydrogenation step also obeys the BEP relation since the HCOOH formation reaction is more endothermic than the CO formation reaction.

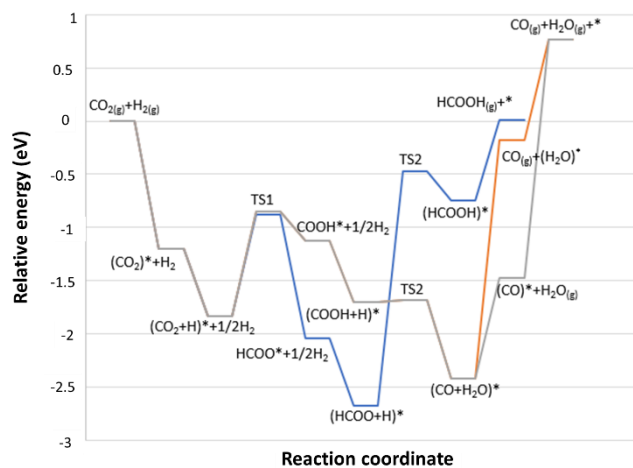


Figure 4. Potential energy profiles of CO₂ hydrogenation to CO and HCOOH on graphene-supported subnanometer Ni₇ cluster.

We compile the potential energy profiles for the CO₂ hydrogenations relative to the gas phase of molecules in **Fig. 4**. From this figure, it can be seen that the selectivity of CO₂ hydrogenation on the Ni₇/graphene system is solely dictated by the

second hydrogenation step because the first step has quite similar activation energies. Since the CO formation has significantly lower activation energy than the HCOOH formation, the CO₂ hydrogenation on the Ni₇/graphene system is more selective toward the RWGS pathway. However, we should also notice that CO removal from the Ni₇ cluster requires quite high desorption energy (> 2eV). This situation raises two possible scenarios. The first one is that the Ni₇ will be poisoned by CO. The second possibility is that the CO might not be the final product of the RWGS pathway. The adsorbed CO might go through another chain of hydrogenation reactions to form other products such as methanol (CH₃OH) or methane (CH₄). These possibilities will be further explored in our future study.

We also compare our results with the case of the Ni(111) surface (Maulana *et al.*, 2019). In the Ni(111) case, the CO₂ hydrogenation reaction is more selective towards the formate pathway. Interestingly, the usage of Ni in the form of subnanometer Ni_x cluster shifts the selectivity of CO₂ hydrogenation reaction towards the RWGS pathway. Unfortunately, the activation energies for the first hydrogenation step on Ni₇/graphene system are still higher than the Ni(111) surface ($E_a^{HCOOH} = 0.55$ eV and $E_a^{COOH} = 0.85$ eV). One of the possible reasons is because the Ni₇ cluster binds CO₂ molecule too strong ($E_{ads}^{CO_2} = -1.20$ eV). The formation of HCOO* and COOH* requires some geometrical reconstructions from the adsorbed CO₂ during the hydrogenation process. These reactions become more sluggish on the Ni₇/graphene system because the very strong CO₂ bidentate adsorption hinders the reconstruction process. The second hydrogenation step on the Ni₇/graphene system for the HCOOH formation is also much higher than the Ni(111) surface ($E_a^{HCOOH} = 0.85$ eV). However, the activation energy for the CO formation step on the Ni₇/graphene system is much lower than the Ni(111) surface ($E_a^{CO_2+H_2O} = 0.25$ eV). This again indicates that the RWGS + CO hydrogenation pathway on the Ni₇/graphene might have good potentials to be further explored.

Conclusions

We study the mechanism of CO₂ hydrogenation to HCOOH and CO on the graphene-supported subnanometer Ni₇ cluster using DFT calculations. We find that this system has quite similar activation energies for the first hydrogenation step of the formate and RWGS pathways. However, the second hydrogenation step for these pathways has very distinct activation energy profiles. The HCOOH formation (formate pathway) has very large activation energy, while the CO formation (RWGS pathway) has negligible activation energy. From this result, we conclude that the CO₂ hydrogenation process on this system is more selective towards the RWGS pathway to produce CO. However, the catalyst might be prone to CO poisoning due to its immense desorption energy. This suggests that the final product for the CO₂ hydrogenation on this system is not CO molecule, and instead, it might be further hydrogenated into different products such as methane or methanol.

Conflict of Interest

We have no conflict to declare.

Acknowledgements

This work is supported by the Ministry of Research, Technology, and Higher Education through the "World Class Research" program. All calculations were performed using High Performance Computing facility in Research Center for Nanosciences and Nanotechnology, Institut Teknologi Bandung.

References

- Abanades, J. C. *et al.* (2017) 'On the climate change mitigation potential of CO₂ conversion to fuels', *Energy and Environmental Science*, 10(12), pp. 2491–2499. doi: 10.1039/c7ee02819a.
- Agusta, M. K. *et al.* (2017) 'Conformational effects on hydrazine and OH coadsorption on Ni(111): A first-principles investigation', *Surface Science*, 664(March), pp. 185–193. doi: 10.1016/j.susc.2017.06.013.
- Agusta, M. K. *et al.* (2019) 'Coadsorption of hydrazine (N₂H₄) and OH on NiZn surface: a DFT-based study', *Surface Science*, p. 121505. doi: <https://doi.org/10.1016/j.susc.2019.121505>.
- Álvarez, A. *et al.* (2017) 'Challenges in the Greener Production of Formates/Formic Acid, Methanol, and DME by Heterogeneously Catalyzed CO₂ Hydrogenation Processes', *Chemical Reviews*, 117(14), pp. 9804–9838. doi: 10.1021/acs.chemrev.6b00816.
- Bronsted, J. N. (1928) 'Acid and Basic Catalysis.', *Chemical Reviews*, 5(3), pp. 231–338. doi: 10.1021/cr60019a001.
- Catapan, R. C. *et al.* (2012) 'DFT study of the water-gas shift reaction and coke formation on Ni(111) and Ni(211) surfaces', *Journal of Physical Chemistry C*, 116(38), pp. 20281–20291. doi: 10.1021/jp302488f.
- Ding, X. *et al.* (2007) 'Interaction of carbon dioxide with Ni(110): A combined experimental and theoretical study', *Physical Review B - Condensed Matter and Materials Physics*, 76(19), pp. 1–12. doi: 10.1103/PhysRevB.76.195425.
- Ding, Xunlei *et al.* (2007) 'Modeling adsorption of CO₂ on Ni(110) surface', *Materials Science and Engineering C*, 27(5-8 SPEC. ISS.), pp. 1355–1359. doi: 10.1016/j.msec.2006.06.024.
- Evans, M. G. and Polanyi, M. (1938) 'Inertia and driving force of chemical reactions', *Transactions of the Faraday Society*, 34(0), pp. 11–24. doi: 10.1039/TF9383400011.
- Giannozzi, P. *et al.* (2009) 'QUANTUM ESPRESSO: A modular and open-source software project for quantum simulations of materials', *Journal of Physics Condensed Matter*, 21(39). doi: 10.1088/0953-8984/21/39/395502.
- Grimme, S. (2006) 'Semiempirical GGA-type density functional constructed with a long-range dispersion correction', *Journal of Computational Chemistry*, 27(15), pp. 1787–1799. doi: 10.1002/jcc.20495.
- Henkelman, G., Uberuaga, B. P. and Jónsson, H. (2000) 'Climbing image nudged elastic band method for finding saddle points and minimum energy paths', *Journal of Chemical Physics*, 113(22), pp. 9901–9904. doi: 10.1063/1.1329672.
- Hohenberg, P. and Kohn, W. (1964) 'Inhomogeneous electron gas', *Physical Review*, 136(3B), pp. B864–B871. doi: 10.1103/PhysRev.136.B864.
- Kätelhön, A. *et al.* (2019) 'Climate change mitigation potential of carbon capture and utilization in the chemical industry', *Proceedings of the National Academy of Sciences of the United States of America*, 166(23), pp. 11187–11194. doi: 10.1073/pnas.1821029116.
- Kohn, W. and Sham, L. J. (1965) 'Self-Consistent Equations Including Exchange and Correlation Effects', *Phys. Rev.*, 140(4A), pp. A1133–A1138. doi: 10.1103/PhysRev.140.A1133.
- Liu, X. M. *et al.* (2003) 'Recent Advances in Catalysts for Methanol Synthesis via Hydrogenation of CO and CO₂', *Industrial and Engineering Chemistry Research*, 42(25), pp. 6518–6530. doi: 10.1021/ie020979s.
- Mahyuddin, M. H. *et al.* (2016) 'Direct Conversion of Methane to Methanol by Metal-Exchanged ZSM-5 Zeolite (Metal = Fe, Co, Ni, Cu)', *ACS Catalysis*, 6(12), pp. 8321–8331. doi: 10.1021/acscatal.6b01721.
- Mahyuddin, M. H. and Yoshizawa, K. (2018) 'DFT exploration of active site motifs in methane hydroxylation by Ni-ZSM-5 zeolite', *Catalysis Science and Technology*, 8(22), pp. 5875–5885. doi: 10.1039/c8cy01441h.
- Maulana, A. L. *et al.* (2019) 'DFT and Microkinetic Investigation of Methanol Synthesis via CO₂ Hydrogenation on Ni(111)-based Surfaces', *Physical Chemistry Chemical Physics*, (111), pp. 1–11. doi: 10.1039/C9CP02970B.
- Mustafa, A. *et al.* (2020) 'Current technology development for CO₂ utilization into solar fuels and chemicals: A review', *Journal of Energy Chemistry*, 49, pp. 96–123. doi: 10.1016/j.jechem.2020.01.023.
- Nugraha *et al.* (2016) 'DFT study of the formate formation on Ni(111) surface doped by transition metals [Ni(111)-M; M=Cu, Pd, Pt, Rh]', in *Journal of Physics: Conference Series*. doi: 10.1088/1742-6596/739/1/012082.
- Peng, G. *et al.* (2012) 'CO₂ hydrogenation to formic acid on Ni(110)', *Surface Science*, 606(13–14), pp. 1050–1055. doi: 10.1016/j.susc.2012.02.027.
- Perdew, J. P., Burke, K. and Ernzerhof, M. (1996) 'Generalized gradient approximation made simple', *Physical Review Letters*, 77(18), pp. 3865–3868. doi: 10.1103/PhysRevLett.77.3865.
- Pradana, M. R. *et al.* (2019) 'Theoretical Study on the Interaction of Graphene-supported Nickel cluster with CO₂ molecule', in *The 8th Asian Physics Symposium*. IOP Publishing.
- Remediakis, I. N., Abild-Pedersen, F. and Nørskov, J. K. (2004) 'DFT study of formaldehyde and methanol synthesis from CO and H₂ on Ni(111)', *Journal of Physical Chemistry B*, 108(38), pp. 14535–14540. doi: 10.1021/jp0493374.
- Saputro, A. G. *et al.* (2016) 'DFT study of adsorption of CO₂ on palladium cluster doped by transition metal', in *Journal of Physics: Conference Series*. doi: 10.1088/1742-6596/739/1/012083.
- Saputro, A. G. *et al.* (2019) 'Theoretical study of CO₂ hydrogenation

to methanol on isolated small Pdx clusters', *Journal of Energy Chemistry*, pp. 79–87. doi: 10.1016/j.jechem.2018.11.005.

Saputro, A. G., Maulana, A. L., Fathurrahman, F., *et al.* (2021) 'Density functional and microkinetic study of CO₂ hydrogenation to methanol on subnanometer Pd cluster doped by transition metal (M= Cu, Ni, Pt, Rh)', *International Journal of Hydrogen Energy*, 46(27), pp. 14418–14428. doi: 10.1016/j.ijhydene.2021.02.009.

Saputro, A. G., Maulana, A. L., Aprilyanti, F. D., *et al.* (2021) 'Theoretical Study of Direct Carbon Dioxide Conversion to Formic Acid on Transition Metal-Doped Subnanometer Palladium Cluster', *Journal of Engineering and Technological Sciences*, 53(4). doi: 10.5614/xxxx.

Saputro, A. G. and Akbar, T. (2017) 'Reaksi Hidrogenasi Metoksida Menjadi Metanol pada Klaster Pd 6 Ni', *Journal of Science and Applicative Technology*, 1(2), pp. 53–57.

Singha, R. K. *et al.* (2019) 'Methane Activation at the Metal-Support Interface of Ni₄-CeO₂(111) Catalyst: A Theoretical Study', *Journal of Physical Chemistry C*, 123(15), pp. 9788–9798. doi: 10.1021/acs.jpcc.8b11973.

Vesselli, E. *et al.* (2008) 'Carbon dioxide hydrogenation on Ni(110)', *Journal of the American Chemical Society*, 130(34), pp. 11417–11422. doi: 10.1021/ja802554g.

Vesselli, E. *et al.* (2010) 'Hydrogen-assisted transformation of CO₂ on nickel: The role of formate and carbon monoxide', *Journal of Physical Chemistry Letters*, 1(1), pp. 402–406. doi: 10.1021/jz900221c.

Wang, S. *et al.* (2005) 'Chemisorption of CO₂ on Nickel Surfaces', *Journal of Physical Chemistry B*, 109, pp. 18956–18963.

Waugh, K. C. (1992) 'Methanol Synthesis', *Catalysis Today*, 15(1), pp. 51–75. doi: [https://doi.org/10.1016/0920-5861\(92\)80122-4](https://doi.org/10.1016/0920-5861(92)80122-4).

Zhang, J. *et al.* (2019) 'Theoretical investigation of loading Ni

clusters on the A-Ga₂O₃ surfaces for photocatalytic hydrogen evolution', *Journal of Energy Chemistry*, 30, pp. 8–18. doi: 10.1016/j.jechem.2018.03.007.